Nat. Hazards Earth Syst. Sci. Discuss., 2, 3965–4010, 2014
www.nat-hazards-earth-syst-sci-discuss.net/2/3965/2014/
doi:10.5194/nhessd-2-3965-2014

Natural Hazards and Earth System Sciences
Open Access
Discussions

Fracture network characterisation of a landslide by electrical resistivity tomography

S. Szalai[1], K. Szokoli[1], A. Novák[1], Á. Tóth[2], M. Metwaly[3,4], and E. Prácser[1]

[1]RCAES HAS, GGI, 9401 Sopron POB 5, Hungary
[2]Department of Physical and Applied Geology, Eötvös Loránd University, Budapest, Hungary
[3]Archaeology department, college of tourism and archaeology, King Saud University, Riyadh, Saudi Arabia
[4]National Research Institute of Astronomy and Geophysics (NRIAG), Cairo, Egypt

Received: 23 April 2014 – Accepted: 15 May 2014 – Published: 5 June 2014

Correspondence to: S. Szalai (szalai@ggki.hu)

Published by Copernicus Publications on behalf of the European Geosciences Union.

Abstract

In contrary to most of the landslide studies which concentrate to the sliding surface in this paper the fracture system of a loess landslide is investigated. The continuity and geometry, orientation and dip of the major fractures are crucial parameters for assessing rock stability and landslide evolution. Rain infiltrating moreover easily into the rock mass through fractures providing lubrication for the material to slide, and increases the self-mass of the material increasing the slumping rate. Fracture maps enable beside of the characterisation of the fractured area the delineation of the endangered area of slow-moving landslides in due time and getting information about its inner structure. For constructing such maps Electrical Resistivity Tomography (ERT) measurements have been carried out using different geoelectric configurations. In spite of the high density of the fractures and their changing physical parameters in function of their water content – which make the interpretation rather difficult – a number of fractures have been detected and more or less well localised. On the basis of the present research the application of the Schlumberger and the Pole-Dipole arrays is recommended to fulfil the aim of the study. The optimised Stummer array is at the same time the only array which presents conductive anomalies (supposedly water filled fractures), as well, and indicates that fractures elongate deep downwards. Because these features seem to be realistic based on field observations or theoretical considerations the Stummer array may be a very good tool for completing e.g. P-Dp measurements. The study area could have been divided by all arrays into differently fractured zones, which assists a lot in understanding the landslide structure and evolution. It was shown, moreover, that in the still passive area there are thick fractures, too, verifying its dangerousness, as well. The ERT results enabled localising the rupture surfaces of future slumps which proved to be distributed uniformly with about 10 m distance between them and predicting mass movements which may prevent the slump along the visible fracture. Similar unidirectional fracture systems could be investigated by the ERT method for any hydrogeological or engineering geological aim.

1 Introduction

A landslide is a downslope movement of a soil or rock which occurs due to local geological and groundwater conditions, extreme weather events, earthquakes and other factors. Cracks at top of a slope indicate the initiation of a new failure or reactivation of a pre-existing one. Landslides can extremely damage facilities, roads, and lifelines but are not usually life-threatening in case of slow movement. Mapping of landslides is therefore important for hazard zonation, planning and protection purposes.

Loess landslide is a typical type of landslides which is widely distributed all over the world. It is e.g. one of the serious geological disasters in and around the loess plateau in northwest of China. It widely distributes, frequently occurs, and causes serious casualties and property losses (Fan et al., 2012). The stabilities of the loess hillside slope before and after excavation were analyzed by Wang et al. (2014). A systematic summary and thorough analysis of the loess-bedrock landslide for reducing disasters caused by loess landslide were given by Fan et al. (2012). The acquired achievements of the loess-bedrock landslide have been summarized on classification, formation mechanism, influencing factors and hazard range, and some main fields are put forward for further researching among others to analyze the main influencing factors and forecast the hazard range of different types of the loess-bedrock landslide.

Geotechnical methods like Core Sampling, Rotary Pressure Sounding (RPS), Cone Penetration Test Undrained (CPTU), Total Sounding (TS), Rotary Sounding, Vane Shear Tests and Pore Pressure Measurements (Solberg et al., 2012) are very significant in studying landslides. CPTU is used to get information on sediment stratification and soil type. RPS is often used to detect quick clay and TS may be used to verify depth to bedrock. Laboratory tests on material from core samples give detailed information on sediment stratification, soil type, too, but also on shear strength, deformation properties, permeability, etc. The engineering geological investigation of a slow moving landslide is presented in Sarah and Daryono (2012). Solberg et al. (2012) combined the geophysical and geotechnical approach.

Remote sensing techniques are also very valuable tools in landslide investigations. Mapping the surface area affected by the landslide is often done by observation of aerial photographs or remote-sensing images (Van Westen, 2004) which indicate the topographical expression of the landslide. However, if the landslide is ancient or little active, its morphologic features and boundaries may have been degraded by erosion and surface observations and measurements have to be supported by reconnaissance at depth (Dikau et al., 1996). The remote sensing techniques like Global Positioning System (GPS), Satellite imagery, RADAR imagery, Stereophotogrammetry, Soft copy photogrammetry are very useful in monitoring the movement of a landslide, too. A summary about the remote sensing techniques applied to study landslides is given by Tofani et al. (2013).

Geodetical methods are also distributed in landslide investigations as it is shown on the example of the in this paper presented site by Újvári et al. (2009) and Bányai et al. (2012, 2013, 2014). GPS observation of landslides has become a firmly established technique over the past decade (e.g. Fukuoka et al., 1995; Jackson et al., 1996; Gili et al., 2000; Malet et al., 2002). It is often used together with deformation measurements (Cencetti et al., 2000; Coe et al., 2003; Corsini et al., 2005).

Physical modelling technique was applied to investigate the initiation and evolution of large scale landslides by Bachmann et al. (2004).

Geophysical methods can be very fruitful for studying landslides, as well. These techniques are summarised e.g. by Bogoslovsky and Ogilvy (1977), McCann and Forster (1990) and Jongmans and Garambois (2007). Landslides and rockfalls can be investigated using seismical (e.g. Bichler et al., 2004; Walter et al., 2012), electrical (e.g. Wisen et al., 2003), electromagnetic (e.g. Méric et al., 2005) and GPR (e.g. Bichler et al., 2004) methods. Joint use of different geophysical methods is also common to improve their productivity, e.g. Bruno and Marillier (1999).

Electrical geophysical measurements were carried out in landslide studies carrying out one-dimensional (1-D) sounding by Caris and Van Asch (1991), Schmutz et al. (2000) and Agnesi (2005) to determine the bedrock depth. Two-dimensional (2-D)

ERT studies were performed to describe the geological boundary and/or determine the slip surface depth by Batayneh and Al-Diabat (2002), Bichler et al. (2004), Demoulin et al. (2003), Lapenna et al. (2005) and Havenith et al. (2000). Beside of 2-D rockslide 3-D slip surface geometry and water flows were investigated by Lebourg et al. (2005). Méric et al. (2005) investigated the lateral boundaries and thickness of a rockslide.

The goal of the applied geophysical techniques therefore used to be mostly the vertical delineation of the sliding volume which supposed to have different physical parameters than that of the non-sliding material. The inner structure of the landslide was less often studied by geophysical methods.

The aim of all aforementioned techniques used to study landslides was therefore the horizontal and/or vertical delineation of the sliding volume, determination of the sediment stratification and soil type, physical parameters of the rocks of the rock massive like shear strength, deformation properties, permeability, etc. Topographical expression of the landslide, monitoring the movement of it, deformation measurements were also carried out. None of these techniques aimed however mapping the fractures which could give a lot of information about the inner structure of a landslide and may enable to forecast future rupture surfaces therefore delineate the endangered areas. It was the goal of the present study by using geoelectric method.

Electric Resistivity Tomography (ERT), the most often used geoelectric method was able to detect fractures (Francese et al., 2009) if the characteristic distance was much larger (about 10 m) than that of supposed to be in the study area (about half meter). Cracks of cm size was studied by Samouëlian et al. (2003) using miniature resistivity imaging. Sentenac and Zielinski (2009) describe a miniaturised ERT technique, too, for mapping the cracking pattern of a clay model and its changes as a function of time. In the scale of the study area application of geoelectric null arrays (Szalai et al., 2002; Szalai and Szarka, 2008; Falco et al., 2013) is known, but it is able to give a map only in a given depth applying only one array length. The application of more array length is in turn rather time consuming. Geoelectric arrays can be used also for determining fracture directions (Taylor and Fleming, 1988), but only with strict limits (Szalai

et al., 2009) especially if there are more fracture directions. Although studying fracture systems would be very useful not only for landslides, but for any fracture system characterisation ERT studies in this scale are not known yet.

Regarding other geophysical techniques Barnhardt and Kayen (2000) detected fractures by ground penetrating radar (GPR), but the resolution of their measurements was only 5 m and the results were questionable. Although the resolution of the GPR results of Jeannin et al. (2006) proved to be very good, their measurements were carried out on a query wall, because the plateau above the cliff is covered by a conductive weathered layer, which decrease drastically the penetration depth of the GPR method. Willenberg et al. (2004) applied borehole radar to locate fractures.

The geotechnical tools would be applicable to map fractures, as well, but they provide information only for point locations. They are moreover expensive and their application is strongly limited by field conditions, like topography, artificial constructions, slide danger and plants, because they make difficult or even impossible the approach of the study area. An economic solution for such problems, the so-called Pressure-Probe method which is a simplified version of the geotechnical instruments is discussed by Szalai et al. (2014). It avoids all aforementioned deficiences of the geotechnical tools.

Our study area differs from most of the investigated landslide areas also beause it seems that there is not any sliding surface. The lack of mass due to chemical processes because of the contact between the Danube water and loess at the bottom of the hill has to lead to the mass movement. This process takes place in a very large depth in comparison with the horizontal distribution of the plateau of the hill which makes its geophysical investigation very complicated. It could moreover help in understanding the landslide evolution, but for making forecast for the future development it has to be insufficient.

Therefore we decided to map the fracture network of the landslide aiming to delineate the endangered area and forecast its future development. Fracture investigations may be important, as well, because although the investigated landslide is supposed to be induced by the Danube water the rain water may severely intensify it infiltrating into the

rock through the fractures. It intensifies in addition the chemical processes leading to more intensive dissolution and mass loss.

Lataste et al. (2003) carried out fracture network investigations in small scale. They used resistivity technique with a small device made of four electrodes, arranged in a square to study the fissures on a damage concrete slab. Lecocq and Vandewalle (2003) found that as soon as a new crack appears, the opening rate of the old one falls by half. On a geology level, Nguyen et al. (2005) suggested a methodology to locate automatically limits or boundaries between faults and layer boundaries in electrical tomography. Samouëlian et al. (2003) have been recorded and displayed by the resistivity equipment all the major vertical cracks, which have been visually observed at the surface of the clay model.

Because of its importance for the present paper the investigation of Sentenac and Zielinski (2009) is discussed in details. They studied 2–4 mm wide fissures in clay with a miniature ERT system. The average distance between the fissures was about 20–24 cm while the electrode distance was 3 cm. The fissures were moreover quasi parallel to each other and at the beginning they were dry and reached the surface. Although all of these parameters are very favorable for the ERT measurements the results were reliable only for the larger fissures. We had to take it into account in the interpretation of our results that is in field conditions the results regarding individual fractures may not be expected to be excellent.

The goal of this paper was to map the fracture system of a loess landslide area by ERT method and to compare the imaging capacity of different ERT configurations. It will be shown that in spite of the difficulties the obtained map enables the delineation of the endangered area and helps understanding the evolution of the investigated landslide.

2 Geological and geomorphological settings

The study area is part of the Baranya Hills (Fig. 1). The monitored bank stretches about 15 km long along the Danube between the Sárköz and Mohács depressions (Moyzes

and Scheuer, 1978) (Fig. 1b) which were formed due to a tectonic movement along the main NE–SW and NW–SE structural lines during Quaternary. It determined also the actual flow direction of the Danube (Moyzes and Scheuer, 1978; Síkhegyi, 2002). Geophysical measurements reinforce that recent tectonic movements are still important in the evolution of the western bank of the Danube near Dunaszekcső (Erdélyi, 1967).

The Triassic–Jurassic limestones basement formations at Dunaszekcső are located 200–250 m below the surface (Szederkényi, 1964; Urbancsek, 1977; Moyzes and Scheuer, 1978; Hegedűs et al., 2008). They are covered by clayey and sandy sediments formed in the Upper Miocene and the Pliocene (12.6 to ∼ 2.6–2.4 Ma; Rónai, 1985) that can be found below about 70 m depth according to borehole data (Moyzes and Scheuer, 1978; Pécsi and Scheuer, 1979). The uppermost 70 m of the sediment sequence are sandy and clayey loess layers with brown to red fossil soils accumulated during the Pleistocene (Fig. 2). The highest point of the bluff (142 m a.s.l.) is at Vár Hill where the southern part of the moving blocks is located (Fig. 3). The flood plain of the Danube is very narrow or missing below southern moving block (SB) at Vár Hill and the northern moving block (NB) at Szent János Hill. The bluff consists of a 20–30 m high vertical loess wall above the 10–20 m high slopes. The slope consists of reworked loess from past landslides and fluvial mud, sand and gravel deposits of the Danube (Fig. 3). The slopes were intensively undercut by the river during each flood event (Moyzes and Scheuer, 1978; Kraft, 2005). The younger loess series on top is less, the older loess below is much more compact (Moyzes and Scheuer, 1978; Scheuer, 1979). The density of the younger loess deposits is around 1.6 g cm^{-3}, while that of the older loess series and the intercalated paleosols is between 2.0–2.1 g cm^{-3}, and that of the Pannonian clays and sands is 2.16 g cm^{-3} (Hegedűs et al., 2008). Ground water flows to the SE during base flow due to the sucking effect of the Danube (Moyzes and Scheuer, 1978).

According to field observations there are tension cracks in the loess complex parallel as well as perpendicular to the Danube's channel. The vertical cracks are clearly visible on the roof of the Töröklyuk cave, a natural cavity on NB. Cracking was probably

provoked by both previous sliding events and recent slumping, but recent tectonic movements may have also influenced this process. Tension cracks have namely appeared also in the apparently intact part of the slope southwards from SB.

Loess corrosion and piping created hollows of various sizes on rock walls (Kraft, 2005). Such process could be activated anytime to open major cracks. Landslides in the studied region are concentrated in areas where relative relief is sufficiently high. This is the situation along the Danube bank where stream undercutting has produced relatively high bluffs. Landslides are highly influenced by the hydrological condition of high bluffs. The water level fluctuation of the Danube is in a range of nearly 10 m. It influences the springs and artesian water at the foot of the bank, which is inundated during higher water stages but draines rapidly during lower water stages (Fábián et al., 2006).

Along the steep bank of the Danube, the Upper Pannonian sediment sequence consisting of alternating permeable and impervious layers is exposed in some places below the Pleistocene or Upper Pliocene loess sequence or the Pliocene red clays. Due to previous slumping and lateral erosion by the Danube, the Upper Pannonian sediments are partly redeposited. The Upper Pannonian sand deposits provide confined aquifers, and their water under pressure locally moistens the overlying past slump deposits, which may led to the reactivation of existing slumps and the generation of new landslides. During spring–summer floods, the Danube inundates the surface to the level of the springs at the base of the bluff, rising the groundwater table. It is noteworthy because slumps and earthslides tend to take place after prolonged high-water stages of the Danube (Domján, 1952; Karácsonyi and Scheuer, 1972; Horváth and Scheuer, 1976; Pécsi et al., 1979; Fábián et al., 2006). According to Cruden and Varnes (1996) the past landslides at Dunaszekcső are historic landslide types, which developed under environmental conditions similar to today's. The numerous mass movements in the past indicate the high landslide susceptibility of this area. The actual study area is presented in Fig. 3, the profiles along which the measurements were carried out in Fig. 4.

3 Former researches in the area

Several regions of Hungary are susceptible to landslides among which the bluff along the west bank of the River Danube between Budapest and Mohács is the most affected (Fig. 1a; Farkas, 1983; Kleb and Schweitzer, 2001; Szabó, 2003). Mass movements have appeared here since the Roman times (Lóczy et al., 1989; Juhász, 1999). The Hungarian Office for Mining and Geology scores more than 20 large landslides happened in the area during the 20th century (Fig. 1b). Recent major movements of the landslides have been studied from engineering geological (Egri and Párdányi, 1968; Kézdi, 1970; Karácsonyi and Scheuer, 1972; Bendefy, 1972; Horváth and Scheuer, 1976; Scheuer, 1979; Pécsi and Scheuer, 1979), geomorphological (e.g. Bulla, 1939; Pécsi, 1971; Pécsi et al., 1979) and hydrogeological (Domján, 1952; Galli, 1952; Schmidt Eligius, 1966) points of view. These studies provided mainly empirical descriptions of the three-dimensional deformations. Geodetic measurements were carried out at Dunaújváros in 1964 after a large slope failure (Egri and Párdányi, 1968; Kézdi, 1970), but the results were only partially published (Kézdi, 1970). There is therefore a lack of monitoring of landslides and their evolution in Hungary by means of both geodetic methods and modern tools (GPS, tiltmeters, etc.) in spite of current problems in this region. In 2007, a 220 m long rupture appeared parallel with the riverbank at Dunaszekcső. The sliding mass was estimated at about $0.3\,m^3 \times 106\,m^3$ and its potential energy which was calculated with a centre of mass of 29 m elevation above the river ($U = mgh$) about 153.6 GJ. The landslide risk endangered some properties and the river navigation. Thus, a GPS network complemented with borehole tiltmeters was established to monitor movements and measure deformations. These measurements can be continuous (e.g. Mora et al., 2003; Puglisi et al., 2005) or discontinuous in time (e.g. Moss et al., 1999; Moss, 2000; Rizzo, 2002; Squarzoni et al., 2005). The network and measurement strategy was designed based on previous investigations of Bányai (2003a, b) and the above-mentioned studies.

4 Method

Electric Resistivity Tomography (ERT) is a technique which aims the determination of the subsurface resistivity distribution. A direct current is passed through the ground between two electrodes, which are called current electrodes (C) and the potential is measured between another two electrodes, so-called potential electrodes (P) located at the ground surface (Fig. 5). From the distortion of the equipotentials one concludes to the subsurface resistivity distribution. If the electrodes are placed equidistantly along a line one can use a computer controlled automatic measuring system which determines the actual current and potential electrodes. In this way a resistivity section can be obtained below the profile. This technique is called two-dimensional ERT because it is assumed that there are resistivity changes only in two directions: horizontally, parallel to the profile and vertically.

According to the position of the electrodes different configurations can be applied (Fig. 5). In the Dipole-Dipole configuration e.g. the order of the electrodes is CCPP and the CC, PP distances are the same while the CP distance is n times of it. In this study Schlumberger (Sch), Pole-Dipole (P-Dp), Dipole-Dipole (Dp-Dp) and an optimised array, the Stummer one have been used (Fig. 5). According to Tabbagh et al. (2007) the Schlumberger array seems to be the most sensitive configuration to vertical resistivity changes (horizontal structures) and more sensitive than other arrays to the horizontal resistivity changes (vertical structures). Its great number of data points and extensive horizontal coverage justified its choice (Sentenac and Zielinski, 2009), too.

The P-Dp and Dp-Dp configurations are also commonly applied to image horizontal resistivity changes and they proved to be better in general than the Schlumberger array in numerical studies for numerous models (Szalai et al., 2013). The Stummer array was created using an optimization process from all traditional four-electrode arrays (Stummer et al., 2004). In the investigations by Szalai et al. (2013) it proved to be the best among the investigated arrays. Field studies using this array are however not known yet with the exclusion the investigations by Stummer et al. (2004) and Nyquist

et al. (2007). Due to the less field experience and the promising numerical results with this array we decided to carry out measurements with it, too, concentrating however first of all to the results of the other, better-known arrays. In the field study the electrode distance of the Stummer array was 1 m in contrary to the 0.5 m distance for the other arrays. Even in this way its section is a bit shorter, 29.5 m in contrary to the 35 m of the other configurations. The ends of the configurations were fitted to each other.

Figure 5 displays the details of all applied configurations. The current electrodes are denoted by stars, the potential electrodes by circles. The applied geometrical parameters are presented in the tables below each configuration while their data points and data number can be seen on the right-hand side of the figure. It is noteworthy that the data number of the Stummer array is about one forth of that of the P-Dp and Dp-Dp arrays. It means it can be measured much faster. In case of the P-Dp array one of the electrodes was in the theoretical infinity, in the practice it was about 60–90 m from the western end of the configuration.

The 10 channels Resistivity-meter Syscal Pro Standard & Switch (72) has been used for carrying out the ERT measurements.

In the ERT data processing finite element method (FEM) was applied for the forward modeling and Smooth model inversion for the inversion process. FEM is a numerical technique for finding approximate solutions to boundary value problems for differential equations. It produces more accurate forward modeling solution than the finite difference method. In the inversion procedure the *Initial Lagrange multiplier or roughness factor* was taken to 100, the *Initial damping factor of resistivity* to 100, the *Vertical/Horizontal roughness ratio* to 5. All other parameters are the basic parameters of the applied EarthImager, Version 1.5.6 (EarthImager, 2006) software. RMS and L_2 norm was used to study the data misfit. L_2 is defined as the sum of the squared weighted data errors (EarthImager, 2006). The RMS is the square root of the mean of the squares of the individual resistivity residuals (difference between predicted and observed resistivities). For most presented arrays RMS was about 2–3 % which is a favorable value. Where it was larger it is going to be discussed.

5 Model of the study area

It is known from former researches that the study area is in fact homogeneous loess in the investigated depth range. It means that electrical resistivity may change only due to structural changes, first of all fracturisation and/or due to the changes of the percentage of moisture which strongly influence the electrical resistivity of the loess (Caicedo et al., 2013). Creating the model it was supposed that the resistivity sections reach the water saturated level which should have low resistivity value (in the range of 20–50 Ωm, Caicedo et al., 2013). In the upper part of the section the homogeneity of the loess should be interrupted only by fractures. The distance of the minor fractures was assumed to be 0.5–1 m based on the characteristic fracture distance on the roof of the Töröklyuk cave which is close to the study area (Kraft, 2005).

Prior to the measurements the fractures supposed to be (I) empty, or (II) filled by loose material (Fig. 6.). If they are empty, but finite length and they are partially filled by water they can be resistive in their upper and conductive in their bottom part (Ia). In case if they are "infinitely" long they are resistive (Ib). If they are filled by loose loess (not as compact as the host rock) certain part of them may be conductive depending on the time of the last rain(s) and the water filtration parameters in the given fractures (II). This complexity could make the data interpretation rather difficult. It would therefore be ideal to carry out measurements after a long dry period (Szalai, 2005) when all fracture generated anomalies are resistive. In our case the measurements should have carried out however after a short rainy period which is not ideal for such kind of measurements.

The precipitation distribution prior to the measurements is presented in Fig. 7. Because of logistic reasons the order of the measurements was: P3, P4, P2, P1, one profile each day on 12–15 November, accordingly. The precipitation of four time periods may influence the state of the fractures. The first one started long time, about 45 days before the measurements, but its 47 mm rainfall was significant. The rainfall 26 days prior the measurements produced 27 mm rainfall, the one 6–8 days before 27 mm all together and in the 3 days directly before the measurements 9 mm rainfall

was recorded. We are going to investigate whether any of these rainfalls influenced the measured results. As it was mentioned earlier if the precipitation does not have measurable influence to the measurements the fractures have to produce higher resistivity values than the unfragmented loess.

It is useful to suppose in the interpretation of the resistivity sections that the fractures are closely vertical. It is well-founded expectation looking at the existing sliding fronts. The fractures are therefore assumed to be vertical layer-like features, and most likely very narrow ones. The observed such anomalies are mostly resistive (red in the green background) and just in some cases conductive. The one e.g. on the first three images of Fig. 8 at 21 m (which elongates close to the surface) is moreover most likely due to the increased water saturation level between the two fractures.

6 Results and interpretation

At first look at the P2 results (Fig. 8.), because it supposed to be the most fractured that is the most characteristic among the investigated ones. It was measured three days after the last rainfall on 11 November.

Based on the Schlumberger, P-Dp and Dp-Dp sections it looks that there are principally three layers: the uppermost about 0.5 m thick layer with a resistivity value of about 100 Ωm, an inhomogeneous layer at 0.5–2 m depth, with resistivity values more than 100 Ωm and a conductive layer below 2–3 m depth with resistivity values less than 50 Ωm. Because the study area is almost homogeneous the resistivity changes were supposed to origin from structural and/or water saturation variations. The green areas in the middle "layer" have been regarded as background and supposed that they describe dry loess with their about 140 Ωm value (13 % water saturation). The uppermost layer may correspond to wetter loess (its 100 Ωm resistivity value corresponds to about 15 % water saturation) due to most likely the rainfall three days ago. The water saturation values in the function of the resistivity values of the loess have been taken from Caicedo et al. (2013). The discontinuity of the second inhomogeneous layer supposed

to appear due to fractures. Most of them look very resistive ones therefore they have to be unloaded or the loess inside of them has to be more or less loose with dry pores. Below this layer the loess seems to be almost entirely saturated. 20–50 Ωm resistivity values correspond to 30 and 18 % water saturation (Caicedo et al., 2013), respectively.

Because the images of the the first three arrays are significantly different from that of the Stummer array in the first step only these images will be discussed. It is well seen that the lower part of the sections does not contain any information about the fractures. The resistive anomaly in the middle of the Dp-Dp section is most likely an artifact, which may be produced by the inversion procedure because it is difficult to explain geologically. There is not any indication moreover to such an anomaly on neither of the other profiles. It seems that below the black thick continuous lines it is not possible to get any information about the fractures. But it is not necessary as it was discussed earlier and to get the surface projection of the fracture distribution it is enough to study the upper half of the section. Due to these reasons only the upper part of the sections will be displayed for the other profiles.

Almost all anomalies in the second layer are resistive ones (orange, red on the images) that is their resistivity values are higher than that of the 140 Ωm background value. This means that the fractures have to be dry making the interpretation much easier.

On the Schlumberger (Sch) image the resistive zones are well separated from each other. They belong to three groups denoted by rectangles on the topmost image (Fig. 8). The first zone, closest to the scarp shows that the loess is very fragmented at the hill edge. Fracture zone 3, with the largest anomaly belongs to the main fracture (MF) which is directly visible on the surface. Fracture zone 2 is almost exactly in the middle between zone 1 and zone 3. It seems that the area from zone 1 to zone 3 which is anyway consolidated is going to snap in the middle of it. The P-Dp and Dp-Dp images look very similar, but they are not so characteristic. While P-Dp zone 1 divides into two sub zones Dp-Dp zone 1 is wider than that of the Sch one. It is remarkable that the anomaly at 21.5 m which is a part of fracture zone 2 seems to elongate even

deeper than the anomaly due to the MF (light blue in the deep blue). The anomalies at 21.5 m and 20 m appear on all images verifying the existence of this fracture pair. The P-Dp image displays more fractures in fracture zone 2, than the Sch image thanks to its better horizontal resolution, but the three fracture zones are still clearly distinguishable, although zone 3 continues to the left even with a deep anomaly at 9 m. This anomaly appears on the Dp-Dp image, as well. It means that there are significant fractures over the MF, too, verifying that this area is also endangered.

Although the Stummer array presents the same fracture zones its fractures elongate deeper especially the MF. It reaches even the bottom of the section that is 6 m deep in contrary to the other images where it seems to deepen into not more than 4 m. It should be studied yet whether it describes the reality. The anomaly at 10 m is also remarkable because it occurs much weaker on the other sections. It does not seem to reach the surface like most of the other anomalies. The shape of the other St anomalies resemble better to the expected, vertically elongated layer. Further field studies are recommended to carry out using this array also because in numerical investigations it proved to be the best one among the investigated arrays (Szalai et al., 2013).

The St array anomalies at 8 m and the P-Dp array anomaly at 21 m are the only clear examples for vertically elongated conductive anomalies, although there are some anomalies which are rather questionable, e.g. the one at 12 m on the Dp-Dp image. It is difficult to decide whether these anomalies are artifacts produced by the inversion process or they are real anomalies. Therefore we are going to focus in the followings on the resistive anomalies which are on the other hand much more numereous.

Because the bottom part of the sections does not give any information about the fractures due to the water saturation in the followings only the upper 2.5–3.5 m of the sections will be presented for all profiles. The separation of the individual fractures has to thus be better achievable, too.

The clearest anomalies whose resistivity values are significantly different from the background value and which are mostly vertically elongated (e.g. the ones at 12 and 21.5 m on the Schlumberger profile on Fig. 9) are denoted by continuous lines on

the next figures (Figs. 9–12). The not so outstanding anomalies which have smaller resistivity contrast to the background value and which are mostly not so elongated vertically will be indicated by dotted lines.

The separation of the fractures is often difficult especially if they are close to each other. It is very favourable at the same time from the point of separation that the fractures reach very close to the surface. It is known from the experiments of Sentenac and Zielinski (2009) that even in modelling and applying an ERT configuration with very small electrode distance the fractures could not be localized precisely especially if the fractures are not perpendicular to the profile. One may not therefore expect perfect results in localization of individual fractures, but it has not to be the aim. It is satisfying and it is possible to detect them and localize more or less precisely and to appreciate their significancy.

All investigated arrays present nearly the same number of fractures (Fig. 9): 18, 20, 20 and 22 the Sch, P-Dp, Dp-Dp and the St arrays, respectively. The Stummer configuration displays therefore a little bit more fractures in spite of its shorter section. The three first images are very similar to each other in particular if one regards the continuous line fractures. The positioning of the dotted line fractures is ambiguous. The Stummer image is significantly different from the other sections. The resistive anomalies, e.g. the one at 7 m, 20 m and 27 m elongate much deeper than on the sections of the other arrays. There are resistive anomalies which start deeper, e.g. the one at 2.5–5 m, or 9 m. The St array is the only array which produce strong conductive anomalies, e.g. the ones at 6, 8, 10 and 23 m. They might be artifacts or loose zones filled by water. The later explanation seems to be more likely, but its verification is complicated. Due to that the imaging properties of the Sch, P-Dp and Dp-Dp arrays seem to be very similar the application of one of them seems to be satisfying, while the St array could complete it with a lot of additive, but more ambiguous information.

From the interpretation of Profile 2 based on Figs. 8 and 9 it can therefore be said that: (1) the anyway homogeneous area consisting mainly of loess can be divided into three layers according to its different state. In the lowest layer the water saturation

decreases the resistivity value, while the unloaded or loose and dry fractures in the middle layer increase the resistivity values making it larger than that of the about 140 Ωm background value. (2) While separation of the individual fractures is rather difficult all images enable dividing the profile into zones more or less fractured. (3) The separation of the individual fractures seems to be a little bit better for the P-Dp and Dp-Dp arrays than for the Schlumberger array. (4) The Stummer image is rather different from the other images. Its anomalies are more elongated vertically and it presents more fractures than the other arrays. It was the only array which indicated conductive anomalies, as well. In spite of the uncertainties which are demonstrated by the high RMS value, too, its further study is higly recommended. (5) The average distance between the fractures in the fractured zones is about 1 m which correlates well with that is seen in the Töröklyuk cave near the study area in the same rock.

The P1 Sch image which describes the South part of the investigated area (Fig. 10) is very similar to the P2 Sch section, disregarding from the more spectacular fracture zone on the still passive side of the MF. The fractures here seem moreover at least as thick as the fractures in the other fracture zones excluding the MF. It is by all means warning. The three first images are very similar to each other. On the basis of them the application of only one of them is recommended for economic reasons.

The P1 Stummer image is a little different from the other P1 images similarly to what was observed on P2 but the differences are not as significant in this case. Although its anomalies are much weaker than those ones for the other arrays, they are more characteristic, resembling more to fractures. The fractures appear again at different locations on the images made by different arrays. The precise localisation of smaller individual fractures does not seem therefore to be achievable. In this case the Stummer array does not present any conductive anomalies. Regarding that this profile was measured on the last day, that is 4 days after the last rainfall it enhances the hypothesis that the P2 conductive anomalies were real anomalies. If they would have been artifacts similar artifacts would most likely appear on P1, as well. The Stummer array was therefore the only array which presented also conductive anomalies in the fractured layer on P2.

The P1 anomalies are not as characteristic as those of the P2 and P3 ones especially on the active side. This area does not seem to be therefore as fractured, which most likely means that it is not as endangered.

The next profile, P4 has been measured in the area which seemed to be stable (Fig. 11) lacking any indications of existence of fractures. This assumption has been quickly verified because a much narrower resistivity scale had to be applied to present the inversion results which refers to small resistivity changes, that is to a quite stabile area. The values were in an extra narrow range for the Schlumberger array. Although there is a most likely loose area close to the slide front, it must not be dangerous regarding the insignificantly small resistivity change. However it is noteworthy that in spite of the small changes the Sch image is very informative. It displays a lot of small fractures which even seem to reach the surface in contrary to those on the earlier discussed figures. Their distribution is much more uniform than on the other figures which may refer to the original loess fragmentation which may even occur without any slide event. The increase in fracturisation at the western end of the profile may occur due to smaller instability close to this edge of the hill.

The P-Dp image displays an almost continuous resistive layer (200–400 Ωm) having a larger resistivity value than that of the dry consolidated loess (less than 160 Ωm). It suggests that the loess is not compact in this layer in this area. There are most likely a lot of small fractures close to each other producing a loose loess mass here.

The Dp-Dp image is again very similar to the P-Dp one, while the Stummer image is again different from the other ones. It presents fewer anomalies which reach the surface like those of the Schlumberger anomalies, but they penetrate deeper. It does not present as high resistivity values as the P-Dp and Dp-Dp arrays do. It displays three weak fracture zones (like the P-Dp array did) two at both end of the profile and one in the middle of it. It refers therefore to the same structure as P1 on the active side, which is different from the Sch P4 image. The P-Dp and Dp-Dp images are between the Sch and St ones from this point of view.

The not as small (40–60 Ωm) resistivity values of the supposed saturated zone (below 3 m e.g. for the Stummer image) in contrary to the 20–25 Ωm values in P2 and P1 profiles suggest, too, that the loess is not as fractured in this area. Less fracture in this depth contains less water namely resulting in a higher resistivity value.

On P3 only P-Dp and Stummer measurements have been carried out (Fig. 12). This profile is determined by two large fractures which are especially well seen on the Stummer image: the MF at 14 m and the fracture at 25 m. Mass movement is likely along the later one preceeding the main event along the MF. The other relatively significant fractures are close to the MF, not in the middle between the two large fractures. The explanation will be given later. The passive area seems to be more stable than on P2 especially on the St image.

The St array presents again conductive anomalies which are now deeper starting from about 1.5 m depth. Regarding that these data were acquired on the second day, one day after the P2 data where there are conductive anomalies close to surface it is possible that these anomalies shows the effect of the water which infiltrated to this depth meantime. The smaller and larger depth of the conductive anomalies on P2 and P3 and the non-existence of them on the other profiles which were measured later suggest downwards fluid movement and therefore also the correctness of the Stummer results according to the conductive anomalies. One should emphase again, that such anomalies have not been presented by any other arrays. These results show, as well, that in the study area rainfall could influence the ERT results only for the next two days. It is not surprising because the filtration has to be very quick along the fractures even if they are not unloaded just filled with loose material. In spite of it to carry out such measurements is still recommended in dry periods to avoid the possibility of data misinterpreation.

The Stummer images are the ones, too, which indicate that the fractures reach very close to the surface. It was verified by direct observation at many positions. Although most of fractures are not visible, they are only covered by vegetation and soil which eroded into them and was fixed by roots.

Summarising the Stummer results they often gave quite different images than the other arrays, although the main characteristics of them, regarding the fracture zones were very similar. It was, however, the only array which presented (1) conductive anomalies, as well; (2) fractures elongating deep downwards; (3) fractures reaching closely to the surface. All of these features seem to be realistic based on field observations or theoretical considerations. It means that the Stummer array seem to be a very good tool for completing e.g. P-Dp measurements even if it has not yet been adequately studied in field applications.

All P-Dp images are displayed together on Fig. 13 to have an oversight about the whole study area. The distance (horizontal) axis of them is placed on the corresponding profile. The resistive, fractured zones are again denoted by rectangles on each section.

The similarity between P1 and P2 is remarkable. Even also the widths of the corresponding zones, which are connected by red arrows, are almost the same disregarding from the one directly on the left of the MF. The corresponding fractured (connected by red arrows) and non-fractured zones (connected by black arrows) seem to describe therefore a quasi parallel fracture system in this region. The fractures are moreover closely parallel both to the edge and the MF.

The same is the situation on the active side of P2 and P3, but their passive side is rather different. The difference is most likely due to the sharp curvature (indicated by a full circle) in the edge at P3. The passive side structure of P3 continues on P4 creating again a closely parallel fracture system in this area whose direction is however different from the direction of the active area on P1, P2 and P3. All areas which can be characterised by a fracture direction are denoted by dotted line rectangles. The fracture system in the northern part of the study area, too, seem to follow the MF's direction, however the correlating part of the sections is too small to be convincing. This is the reason that there the arrows are denoted by dashed lines.

Both the MF and the other fractures elongate parallel with the hill edge although the MF approaches to the edge in North. The dotted line which connects the inflexion points

(denoted by full cirles) of the MF and the edge separates well the areas characterised by different fracture directions.

According to the ERT measurements it was therefore possible to separate each profiles into more or less fractured zones and to correlate them with each other. The corresponding zones determine the characteristic fracture directions in the given areas making possible the separation of the whole area into two subareas. It was shown that the fracture directions in these areas correlate well with both the MF and the hill edge.

A possible interpretation of the fracture zone distribution is presented on Fig. 14 showing only the middle, most characteristic part of the study area. The first mass movement which took part in creating the present topography of the study area is representated by the *present edge* (right continuous line arrow).

The fracture along which the next mass movement is expected is recognised at 32 m on P2 and supposed to be outside of P3 (right dotted line arrow). A movement may happen here any time therefore it is called *any time edge*.

From it in about 10 m distance in western direction there is another fracture zone. Although it is actually much less significant than the MF (it is not visible on the surface and its ERT anomaly is significantly less) a slumping may happen there before the slumping along the MF. It is therefore called *near-future edge*. Its role in the near-future is supposed because slumpings used to happen in about uniform segments and the characteristic distance between the fractured zones proved to be about 10 m in the study area.

The next fracture zone, even the next fracture along which slumping is expected is the one which is well visible on the surface and well presented on the ERT images. It is called *future edge*. The names of the actual fracture zones refer to the expected time order when along them a mass movement is expected to take place.

The fracture zones on P2 and P3 were ordered to each other, too, similarly to the edges. P3 does not include fracture zone 1, it is namely more far from the edge and its width is moreover smaller there than on P2 (4 m vs. 6 m).

Fracture zone 4 is at the same time not part of P2. It is in turn very important because it shows that even over the MF, in the still passive area well developed fracture zones can be found. They are recognisable on all profiles more or less characteristically (Fig. 13). Their anomalies are even not less characteristic those of the other ones. We suppose therefore that it is the location along which slumping is going to happen after the slump along the MF. This is why its strongest anomaly is called *far-future* edge. It is also in the characteristic distance of about 10 m from the MF like the *near-future edge* on its other side. On the basis of these results it can be expected that the ERT would be able to present fracture zones in the western continuation of the profiles, as well, enabling the delineation of the endangered area.

7 Conclusions

Former landslide studies focused mainly on the sliding surface or eventually to the layering of it. In this paper the characterisation of the fracture system of a landslide and the delineation of the endangered area was the goal by using different Electrical Resistivity Tomography (ERT) configurations. In spite of the difficulties because of the high density of fractures and their various structural and physical conditions a number of fractures have been recognised and more or less well localised. Fracture zones proved to be detectable more unambiguously enabling map them.

The fractures could not have been observed at large depth due to the water saturation of the host rock below a given depth. On the basis of the existing scarps, however, they are expected to be perpendicular to the surface of the study area to at least 10–20 m depth. It means that the surface projection of the fractures is enough to describe the fracturing in this whole depth domain. It is known from field observations that the fractures reach very close to the surface. They are often covered only by vegetation and a thin layer (10–20 cm) of soil.

The capacity of different ERT configurations for characterising such a fracture system has been compared, as well. The Dipole-Dipole and Pole-Dipole results proved to be

very similar, therefore the application of the little bit less effective one, the Dp-Dp array seems to be needless. The application of the Schlumberger and Pole-Dipole arrays is recommended. The optimised Stummer array often produced different images than the other arrays, although the main characteristics of all of them, regarding the fracture zones have been very similar. The Stummer array was, however, the only array which presented (1) conductive anomalies, as well; (2) fractures elongating deep downwards; (3) fractures reaching closely to the surface. All of these features seem to be realistic based on field observations or theoretical considerations. It means that the Stummer array may be a very good tool for completing e.g. P-Dp measurements even if its field applicability has not yet been adequately studied.

On the basis of the ERT results the study area could have been divided into differently fractured zones. The detection of smaller individual fractures is more complicated and their precise localisation is very difficult.

The interpretation of the fractured zones proved to be very useful for understanding the landslide evolution. It was shown that they follow each other in about 10 m distance forecasting the rupture surfaces of future mass movements. Large fractures have also been detected in the still passive area demonstrating its dangerousness. The ERT method proved therefore to be a tool which enables the delineation of endangered areas in due time for slow-moving landslides. The map which is made using ERT sections verifies that the fracture system is nearly parallel to the hill edge. It was shown, as well, that the southern and northern parts of the study area are not as much endangered than the middle part of it, in spite of that there are fractures, as well.

Such investigations are recommended to carry out in dry periods otherwise the target may have various physical parameters due to its possible water content making the interpretation more complicated. Although this study has been carried out on a loess landslide similar ERT investigations could be applied on any landslides or for any other geological problems where the fractures reach close to the surface and are quasi parallel.

Acknowledgements. S. Szalai, one of the authors of this paper is the grantee of the János Bolyai Scholarship. We would also like to express our thanks to Csaba Molnár for his collaboration in the field survey and data processing.

References

Agnesi, V., Camardab, M., Conoscentia, C., Di Maggio, A., Dilibertoc, I., Madoniac, P., and Rotiglianoa, E.: A multidisciplinary approach to the evaluation of the mechanism that triggered the Cerda landslide, (Sicily, Italy), Geomorphology, 65, 101–116, 2005.

Bachmann, D., Bouissou, S., and Chemenda, A.: Influence of weathering and pre-existing large scale fractures on gravitational slope failure: insights from 3-D physical modelling, Nat. Hazards Earth Syst. Sci., 4, 711–717, doi:10.5194/nhess-4-711-2004, 2004.

Bányai, L.: Geodynamic Investigations Along the Mecsek-Fault in Hungary Using Precise Geodetic Devices, Dept. of Civil Engineering, Patras University, Patras, 65–70, 2003a.

Bányai, L.: Stability Investigations of the High Bank of River Danube in the Area of Dunaföldvár, Dept. of Civil Engineering, Patras University, Patras, 265–271, 2003b.

Bányai, L., Újvári, G., and Mentes, G.: Kinematics and dynamics of a river bank failure determined by integrated geodetic observations – case study of Dunaszekcső Landslide, Hungary, Proceiding of the Annual International Conference on Geological & Earth Sciences (GEOS 2012), Singapore, 36, 51–54, 2012.

Bányai, L., Újvári, G., and Mentes, G.: A dunaszekcsői magaspartcsuszamlás geodéziai megfigyelése, Geodézia és Kartográfia, 65, 7–11, 2013.

Bányai, L., Újvári, G., Mentes, G., Kovács, M., Czap, Z., Gribovszki, K., and Papp, G.: Recurrent landsliding of a high bank at Dunaszekcső, Hungary: geodetic deformation monitoring and finite element modeling, Geomorphology, 210, 1–13, 2014.

Barnhardt, W. A. and Kayen, R. E.: Radar structure of earthquake-induced, coastal landslides in Anchorage, Alaska, Environ. Geosci., 7, 38–45, 2000.

Batayneh, A. T. and Al-Diabat, A. A.: Application of a two-dimensional electrical tomography technique for investigating landslides along the Amman-Dead Sera Highway, Jordan. Env. Geol., 42, 399–403, 2002.

Bendefy, L.: A dunaföldvári partcsuszamlás (The Dunaföldvár landslide), Földrajzi Közlemények, 20, 1–17, 1972.

Bichler, A., Bobrowsky, P., Best, M., Douma, M., Hunter, J., Calvert, T., and Burns, R.: Three-dimensional mapping of a landslide using a multi-geophysical approach: the Quesnel Forks landslide, Landslides, 1, 29–40, 2004.

Bogoslovsky, V. A. and Ogilvy, A. A.: Geophysical methods for the investigation of landslides, Geophysics, 42, 562–571, 1977.

Bruno, F. and Marillier, F.: Test of high-resolution seismic reflection and other geophysical techniques on the boup landslide in the Swiss Alps, Eng. Geol., 52, 113–120, 1999.

Bulla, B.: Teraszvizsgálatok Budapest és Adony között (Investigations of terraces between Budapest and Adony), Földrajzi Közlemények, 63, 92–107, 1939.

Caicedo, B., Murillo, C., Hoyos, L., Julio Colmenares, E., and Berdugo, I. R.: Advances in Unsaturated Soils, Taylor and Francis Group, London, 165–169, 2013.

Caris, J. P. T. and Van Asch, T. W. J.: Geophysical, geotechnical and hydrological investigations of a small landslide in the French Alps, Eng. Geol., 31, 249–276, 1991.

Cencetti, C., Conversini, P., Radicioni, F., Ribaldi, C., Selli, S., and Tacconi, P.: The evolution of Montebestia landslide (Umbria, Central Italy), site investigations, in-situ tests and GPS monitoring, Phys. Chem. Earth, 25, 799–808, 2000.

Coe, J. A., Ellis, W. L., Godt, J. W., Savage, W. Z., Savage, J. E., Michael, J. A., Kibler, J. D., Powers, P. S., Lidke, D. J., and Debray, S.: Seasonal movement of the Slumgullion landslide determined from Global Positioning System surveys and field instrumentation, July 1998–March 2002, Eng. Geol., 68, 67–101, 2003.

Corsini, A., Pasuto, A., Soldati, M., and Zannoni, A.: Field monitoring of the Corvara landslide (Dolomites, Italy) and its relevance for hazard assessment, Geomorphology, 66, 149–165, 2005.

Cruden, D. M. and Varnes, D. J.: Landslide types and processes, in: Landslides: Investigation and Mitigation, Special Report, vol. 247, edited by: Turner, A. K. and Schuster, R. L., Transportation Research Board, National Research Council, National Academy Press, Washington, D.C., 36–75, 1996.

Demoulin, A., Pissart, A., and Schroeder, C.: On the origin of late Quaternary palaeolandslides in the Liège (E Belgium) area, Int. J. Earth Sci., 92, 795–805, 2003.

Dikau, R., Brundsen, D., Schrott, L., and Ibsen, M.-L.: Landslide Recognition: Identification, Movement and Causes, Wiley, Chichester, UK, 274 pp., 1996.

Domján, J.: Középdunai magaspartok csúszásai (Slides of the bluffs along the middle reach of the River Danube), Hidrológiai Közlöny, 32, 416–422, 1952.

EarthImager: 2-D Resistivity and IP Inversion Software, Instruction Manual, Advanced Geosciences Inc., Austin, Texas, 137 pp., 2006.
Egri, G. and Párdányi, J.: Dunaújvárosi magaspartok állékonyság vizsgálata (Stability investigations of the high banks at Dunaújváros), Mûszaki Tervezés, 7, 19–24, 1968.
Erdélyi, M.: A Duna-Tisza közének vízföldtana (Hydrogeology of the Danube-Tisza Interfluve), Hidrológiai Közlöny, 47, 331–340, 1967.
Fábián, S. Z.Á., Kovács, J., Lóczy, D., Schweitzer, F., Varga, G., Babák, K., Lampért, K., and Nagy, A.: Geomorphologic hazards in the Carpathian foreland, Tolna County (Hungary), Studia Geomorphologica Carpatho-Balcanica, 40, 107–118, 2006.
Falco, P., Negro, F., Szalai, S., and Milnes, E.: Fracture characterisation using geoelectric null-arrays, J. Appl. Geophys., 93, 33–42, 2013.
Fan, C., Liang, S., and Ma, X.: Research Advances on the Loess-Bedrock Landslide in China, Asia Pacific Conference on Environmental Science and Technology, Advances in Biomedical Engineering, Vol. 6, Kuala Lump, Malaysia, 2012.
Farkas, J.: Agyagok réteghatárán bekövetkező felszínmozgások (Surface mass movements occurring along the boundaries of clay layers), Mélyépítéstudományi Szemle, 8, 355–361, 1983.
Francese, R., Mazzarini, F., Bistacchi, A., Morelli, G., Pasquarè, G., Praticelli, N., Robain, H., Wardell, N., and Zaja, A.: A structural and geophysical approach to the study of fractured aquifers in the Scansano-Magliano in Toscana Ridge, southern Tuscany, Italy, Hydrogeol. J., 17, 1233–1246, 2009.
Fukuoka, H., Kodama, N., Sokobiki, H., and Sassa, K.: GPS monitoring of landslide movement, Proceedings of the International Sabo Symposium, Tokyo, 1995.
Galli, L.: A dunai és balatoni magaspartok állékonyságának törvényszerűségei (The rules of the stability of high bluffs along the Danube and Lake Balaton), Hidrológiai Közlöny, 32, 409–415, 1952.
Gili, J. A., Corominas, J., and Rius, J.: Using Global Positioning System techniques in landslide monitoring, Eng. Geol., 55, 167–192, 2000.
Havenith, H. B., Jongmans, D., Abdrakmatov, K., Trefois, P., Delvaux, D., and Torgoev, A.: Geophysical investigations on seismically induced surface effects, case study of a landslide in the Suusamyr valley, Kyrgyzstan, Surv. Geophys., 21, 349–369, 2000.

Hegedűs, E., Kovács, A. C., and Fancsik, T.: A megcsúszott dunaszekcsői löszfal aktív és passzív szeizmikus vizsgálata, (Active and passive seismic investigation of the slipped loess bluff at Dunaszekcső), ResearchReport of the Eötvös Loránd Geophysical Institute, Budapest, Hungary, 20 pp., 2008.
Horváth, Z. and Scheuer, G.: A dunaföldvári partrogyás mérnökgeológiai vizsgálata, (Engineering geological investigation of the bank collapse at Dunaföldvár), Földtani Közlöny, 106, 425–440, 1976.
Jackson, M. E., Bodin, P. W., Savage, W. Z., and Nel, E. M.: Measurement of local velocities on the Slumgullion landslide using the Global Positioning System, in: The Slumgullion Earth Flow: a Large-Scale Natural Laboratory, edited by: Varnes, D. J. and Savage, W. Z., US Geol. Surv. Bull., 2130, 93–95, 1996.
Jeannin, M., Garambois, S., and Jongmans, D. G.: Multiconfiguration GPR measurements for geometric fracture characterization in limestone cliffs (Alps), Geophysics, 71, B85–B92, 2006.
Jongmans, D. and Garambois, S.: Geophysical investigation of landslides: a review, B. Soc. Geol. Fr., 178, 101–112, 2007.
Juhász, Á.: A klimatikus hatások szerepe a magaspartok fejlődésében (Role of climatic effects in the development of high banks), Földtani Kutatás, XXXVI, 14–20, 1999.
Karácsonyi, S. and Scheuer, G.: A dunai magaspartok építésföldtani problémái (Engineering geological problems of high banks along the Danube), Földtani Kutatás, 15, 71–83, 1972.
Kézdi, Á.: A dunaújvárosi partrogyás (The bank collapse at Dunaújváros), Mélyépítéstudományi Szemle, 20, 281–297, 1970.
Kleb, B. and Schweitzer, F.: A Duna csuszamlásveszélyes magaspartjainak településkörnyezeti hatásvizsgálata (Assessment of the impact of landslide prone high banks on urban environment along the River Danube), in: Földtudományok és a földi folyamatok kockázati tényezői, edited by: Ádám, A. and Meskó, A., Bp. MTA, 169–193, 2001.
Kraft, J.: A dunaszekcsői Töröklyuk kialakulása és fennmaradása (Evolution and survival of the Töröklyuk cave at Dunaszekcső), Mecsek Egyesület Évkönyve a 2004-es egyesületi évről, Új Évfolyam, 8, 133–153, 2005.
Lapenna, V., Lorenzo, P., Perrone, A., Piscitelli, S., Rizzo, E., and Sdao, F.: 2-D electrical resistivity imaging of some complex landslides in Lucanian Apennine chain, southern Italy, Geophysics, 70, B11–B18, 2005.

Lataste, J. F., Sirieix, C., Breysse, D., and Frappa, M.: Electrical resistivity measurement applied to cracking assessment on reinforced concrete structures in civil engineering, NDT E. Int., 36, 383–394, 2003.
Lebourg, T., Binet, S., Tric, E., Jomard, H., and El Bedoui, S.: Geophysical survey to estimate the 3-D sliding surface and the 4-D evolution of the water pressure on part of a deep seated landslide, Terra Nova, 17, 399–406, 2005.
Lecocq, N. and Vandewalle, N.: Dynamics of crack opening in a one-dimensional desiccation experiment, Phys. A, 321, 431–441, 2003.
Lóczy, D., Balogh, J., and Ringer, Á.: Landslide hazard induced by river undercutting along the Danube, in: Geomorphological Hazards, edited by: Embleton, C., Federici, P. R. and Rodolfi, G., Supplements of Geografia Fisica e Dinamica Quaternaria, 2, 5–11, 1989.
Malet, J. P., Maquaire, O., and Calais, E.: The use of Global Positioning System techniques for the continuous monitoring of landslides: application to the Super-Sauze earthflow (Alpes-de-Haute-Provence, France), Geomorphology, 43, 33–54, 2002.
McCann, D. M. and Forster, A.: Reconnaisance geophysical methodsin landslide investigations, Eng. Geol., 29, 59–79, 1990.
Meric, O., Garambois, S., Jongmans, D., Wathelet, M., Chatelain, J. L., and Vengeon, J. M.: Application of geophysical methods for the investigation of the large gravitational mass movement of Séchilienne, France, Can. Geotech. J., 42, 1105–1115, 2005.
Mora, P., Baldi, P., Casula, G., Fabris, M., Ghirotti, M., Mazzini, E., and Pesci, A.: Global Positioning Systems and digital photogrammetry for the monitoring of mass movements: application to the Ca'di Malta landslide (northern Apennines, Italy), Eng. Geol., 68, 103–121, 2003.
Moss, J. L.: Using the Global Positioning System to monitor dynamic ground deformation networks on potentially active landslides, Int. J. Appl. Earth Obs., 2, 24–32, 2000.
Moss, J. L., McGuire, W. J., and Page, D.: Ground deformation monitoring of a potential landslide at La Palma, Canary Islands, J. Volcanol. Geoth. Res., 94, 251–265, 1999.
Moyzes, A. and Scheuer, G.: A dunaszekcsői magaspart mérnökgeológiai vizsgálata (Engineering geological investigation of the high bank at Dunaszekcső), Földtani Közlöny, 108, 213–226, 1978.
Nguyen, F., Garambois, S., Jongmans, D., Pirard, E., and Loke, M. H.: Image processing of 2-D resistivity data for imaging faults, J. Appl. Geophys., 57, 260–277, 2005.

Nyquist, J. E., Peake, J. S., and Roth, M. J. S.: Comparison of an optimized resistivity array with dipole-dipole soundings in karst terrain, Geophysics, 72, F139–F144, 2007.
Pécsi, M.: Az 1970 évi dunaföldvári földcsuszamlás (The Dunaföldvár landslide in 1970), Földrajzi Értesítő, 20, 233–238, 1971.
Pécsi, M. and Scheuer, G.: Engineering geological problems of the Dunaújváros loess bluff, Acta Geologica Hungarica, 22, 345–353, 1979.
Pécsi, M., Schweitzer, F., and Scheuer, G.: Engineering geological and geomorphological investigations of landslides in the loess bluffs along the Danube in the Great Hungarian Plain, Acta Geologica Hungarica, 22, 327–343, 1979.
Puglisi, G., Bonaccorso, A., Mattia, M., Aloisi, M., Bonforte, A., Campisi, O., Cantarero, M., Falzone, G., Puglisi, B., and Rossi, M.: New integrated geodetic monitoring system at Stromboli volcano (Italy), Eng. Geol., 79, 13–31, 2005.
Rizzo, V.: GPS monitoring and new data on slope movements in the Maratea Valley (Potenza, Basilicata), Phys. Chem. Earth, 27, 1535–1544, 2002.
Rónai, A.: The quaternary of the Great Hungarian Plain, in: Loess and the Quaternary, edited by: Pécsi, M., Akadémiai Kiadó, Budapest, 51–63, 1985.
Samouëlian, A., Cousin, I., Richard, G., Tabbagh, A., and Bruan, A.: Electrical resistivity imaging for detecting soil cracking at the centimetric scale, Soil Sci. Soc. Am. J., 67, 1319–1326, 2003.
Sarah, D. and Daryono, M. R.: Engineering geological investigation of slow moving landslide in Jahiyang Village, Salawu, Tasikmalaya Regency, Indones. J. Geol., 7, 27–38, 2012.
Scheuer, G.: A dunai magaspartok mérnökgeológiai vizsgálata (Engineering geological investigation of the high banks of the Danube), Földtani Közlöny, 109, 230–254, 1979.
Schmidt, E. R.: A dunaújvárosi 1964, évi partomlás (The landslip at Dunaújváros in 1964), MÁFI Évi Jelentése 1964-ről (Annual Report of the Geological Institute of Hungary from the year 1964), MÁFI, Budapest, Hungary, 1966.
Schmutz, M., Albouy, Y., Guérin, R., Maquaire, O., Vassal, J., Schott, J. J., and Descloîtres, M.: Joint electrical and time domain electromagnetism (TDEM) data inversion applied to the Super Sauze earthflow (France), Surv. Geophys., 21, 371–390, 2000.
Sentenac, P. and, Zielinski, Ć. M.: Clay fine fissuring monitoring using miniature geo-electrical resistivity arrays, Environ Earth Sci., 59, 205–214, doi:10.1007/s12665-009-0017-5, 2009.

Síkhegyi, F.: Active structural evolution of the western and central parts of the Pannonian basin: a geomorphological approach, EGU Stephan Mueller Special Publication Series, 3, 203–216, 2002.
Solberg, I. L., Hansen, L., Ronning, J. S., Haugen, E. D., Dalsegg, E., and Tonnesen, J. F.: Combined geophysical and geotechnical approach to ground investigations and hazard zonation of a quick clay area, mid-Norway, B. Eng. Geol. Environ., 71, 119–133, 2012.
Squarzoni, C., Delacourt, C., and Allemand, P.: Differential single-frequency GPS monitoring of theLa Valette landslide (French Alps), Eng. Geol., 79, 215–229, 2005.
Stummer, P., Maurer, H., and Green, A. G.: Experimental design: electrical resistivity data sets that provide optimum subsurface information, Geophysics, 69, 120–139, 2004.
Szabó, J.: The relationship between landslide activity and weather: examples from Hungary, Nat. Hazards Earth Syst. Sci., 3, 43–52, doi:10.5194/nhess-3-43-2003, 2003.
Szalai, S.: Geoelectric Investigation of a Multidirectional Fissure System in a Karstic Area, Near Surface 2005, Palermo, Italy, 2005.
Szalai, S. and Szarka, L.: On the classification of surface geoelectric arrays, Geophys. Prospect., 56, 159–175, 2008.
Szalai, S., Szarka, L., Prácser, E., Bosch, F., Müller, I., and Turberg, P.: Geoelectric mapping of near-surface karstic fractures by using null-arrays, Geophysics, 67, 1769–1778, 2002.
Szalai, S., Kósa, I., Nagy, T., and Szarka, L.: Effectivity enhancement of azimuthal geoelectric measurements in determination of multiple directions of subsurface fissures, on basis of analogue modelling experiments, 15th European Meeting of Environmental and Engineering Geophysics, Dublin, Ireland, 2009, Proceedings & Exhibitors' Catalogue Near Surface 2009, 25 pp., 2009.
Szalai, S., Koppán, A., Szokoli, K., and Szarka, L.: Geoelectric imaging properties of traditional arrays and of the optimised Stummer configuration, Near Surf. Geophys., 11, 51–62, 2013.
Szalai, S., Szokoli, K., Tóth, Á., and Metwaly, M.: Mapping the fracture system of a landslide by pressure probe method, 76th EAGE Conference and Exhibition, Amsterdam, 2014a.
Szalai, S., Szokoli, K., Kis, Á., Metwaly, M., and Lemperger, I.: Increasing the effectiveness of electrical resistivity tomography using γ11n arrays, Geophys. Prospect., submitted, 2014b.
Szederkényi, T.: A baranyai Duna menti mezozoós szigetrögök földtani viszonyai (Geological conditions of the Mesozoic blocks along the River Danube in county Baranya), Földtani Közlöny, 94, 27–32, 1964.

Tabbagh, J., Samouelian, A., and Cousin, I.: Numerical modelling of direct current electrical resistivity for the characterisation of cracks in soils, J. Appl. Geophys., 62, 313–323, 2007.
Taylor, R. W. and Fleming, A. H.: Characterizing jointed systems by azimuthal resistivity surveys, Ground Water, 26, 464–474, 1988.
Tofani, V., Segoni, S., Agostini, A., Catani, F., and Casagli, N.: Technical Note: Use of remote sensing for landslide studies in Europe, Nat. Hazards Earth Syst. Sci., 13, 299–309, doi:10.5194/nhess-13-299-2013, 2013.
Újvári, G., Mentes, Gy., Bányai, L., Kraft, J., Gyimóthy, A., and Kovács, J.: Evolution of a bank failure along the River Danube at Dunaszekcső, Hungary, Geomorphology, 109, 197–209, 2009.
Urbancsek, J.: Magyarország mélyfúrású kútjainak katasztere VII, Cadastre of the deep-drilling wells in Hungary VII, 268, 1977.
Van Westen, C. J.: Geo-Information tools for landslide risk assessment: an overview of recent developments, in: Proc. 9th International. Symp. Landslides, Rio de Janeiro, Brazil, Balkema, Rotterdam, 39–56, 2004.
Walter, M., Schwaderer, U., and Joswig, M.: Seismic monitoring of precursory fracture signals from a destructive rockfall in the Vorarlberg Alps, Austria, Nat. Hazards Earth Syst. Sci., 12, 3545–3555, doi:10.5194/nhess-12-3545-2012, 2012.
Wang, J. J., Liang, I. Y., Zhang, I. H. P., Wu, I. Y., and Lin, I. X.: A loess landslide induced by excavation and rainfall, Landslides, 11, 141–152, doi:10.1007/s10346-013-0418-0.110418-0, 2014.
Willenberg, H., Evans, K. F., Eberhardt, E., Loew, S., Spillmann, T., and Maurer, H. R.: Geological, geophysical and geotechnical investigations into the internal structure and kinematics of an unstable, complex sliding mass in crystalline rock, Proc. 9th International. Symp. Landslides, Rio de Janeiro, Brazil, Balkema, Rotterdam, 489–494, 2004.
Wissen, R., Christiansen, A. V., Auken, E., and Dahlin, T.: Application of 2-D laterally constrained inversion and 2-D smooth inversion of CVES resistivity data in a slope stability investigation, in: Proc. 9th Meeting Env. Eng. Geophys., Prague, Czech Republic, EAGE Publications, Houten, the Netherlands, 2003.

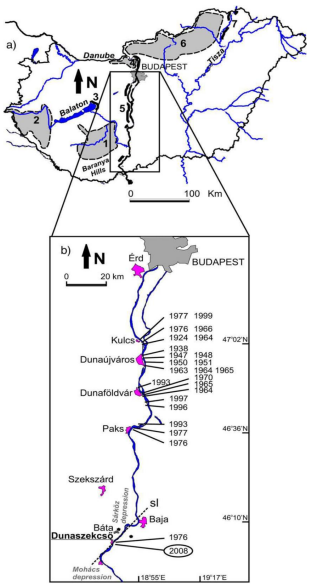

Figure 1. Landslide hazard in Hungary. **(a)** Landslide endangered areas (after Farkas, 1983; Juhász, 1999 and Szabó, 2003). 1. Zselic and Baranya–Tolna Hills; 2. Zala Hills; 3. high banks at Lake Balaton; 4. Visegrád Mountains and terraced region along the Danube; 5. high banks along the Danube; 6. North Hungarian Mountains and Hills; 7. Zemplén Mountain and high banks along the River Hernád. Black coarse lines denote the high banks along the Lake Balaton, the River Danube and the River Hernád. **(b)** Large landslides in the 20th century along the high bank of Danube between Budapest and Mohács (after Juhász, 1999; Kleb and Schweitzer, 2001). Locations and years of the landslides are shown. Black stars indicate local outcropping blocks of Triassic limestone; sl = structural line.

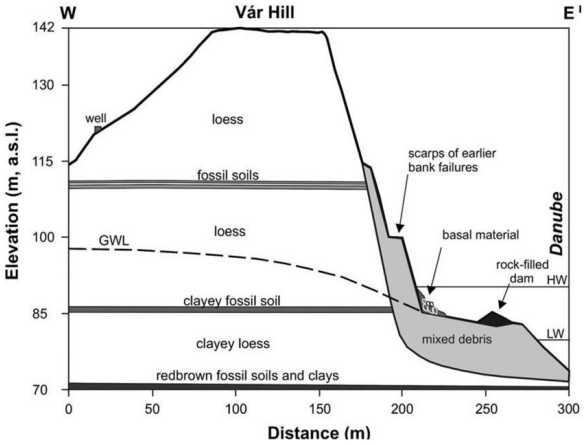

Figure 2. Geological cross-section of the high bank at Dunaszekcső (after Moyzes and Scheuer, 1978; Pécsi et al., 1979; Kraft, 2005). Elevation and distance were derived from the digital terrain model which was provided by geodetic measurements of 433 points. Vertical exaggeration: ×3. GWL = ground water level (measured in a well in July 2008); HW = highest water; LW = lowest water.

Figure 3. (a) The rock mass which has already been slipped looking from South, from the study area. **(b)** The quasi vertical wall along the collapse. The arrow indicates the research area. **(c)** The study area from western direction with tapes along many profiles and with river Danube in the background. The profiles are closely west–east orientated. The red dotted line shows the main fracture which can be directly seen from the opposite direction. The wall is in about 6 m distance from the East end of the tapes. **(d)** The main fracture from East direction with profiles S4–10. The main crack branches off here. In the background the area which have been cultivated. The long profile (P2) elongated between the two wine yards in line S10.

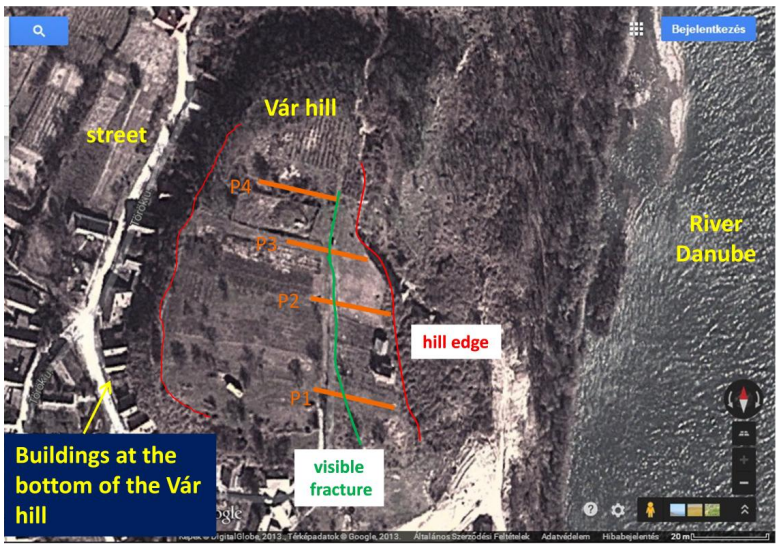

Figure 4. Google image of the research area with the Pre-P profiles. Yellow solid line: main fracture. Yellow dotted line: assumed large fractures outside of the active area attaching both the P1 and P2 profiles. Yellow curve: the actual wall.

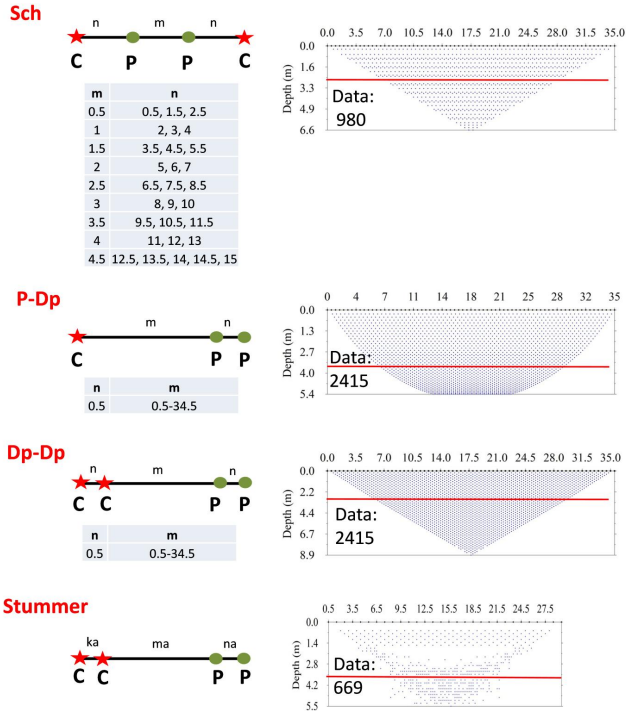

Figure 5. Left side: the applied electrode configurations. Stars: current electrodes (C); circles: potential electrodes (P). In the tables below each configurations the applied geometrical parameters are presented. In the right column the data coverage of them and number of data points can be seen. For the *k*, *m* and *n* parameters of the Stummer array see Stummer et al. (2006). Red lines show the part of the sections which have been presented (above them).

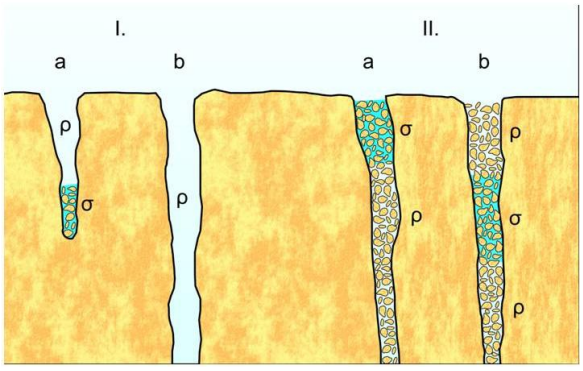

Figure 6. Scheme of the fractures with the possible fillings and the corresponding resistivity values. The regions denoted by "ρ" behave like resistive bodies, while those ones denoted by "σ" behave like conductive bodies. The brown spots indicate loess particles, the blues ones occurrence of water. In case I. the fracture is filled by air, in case II. by loess particles. IIa. is an image just after a rainfall, IIb. is an image supposed to get somewhat later.

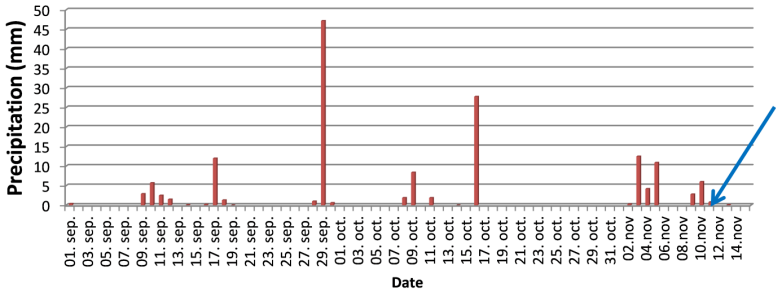

Figure 7. Precipitation prior the measurements. The first field day is indicated by arrow.

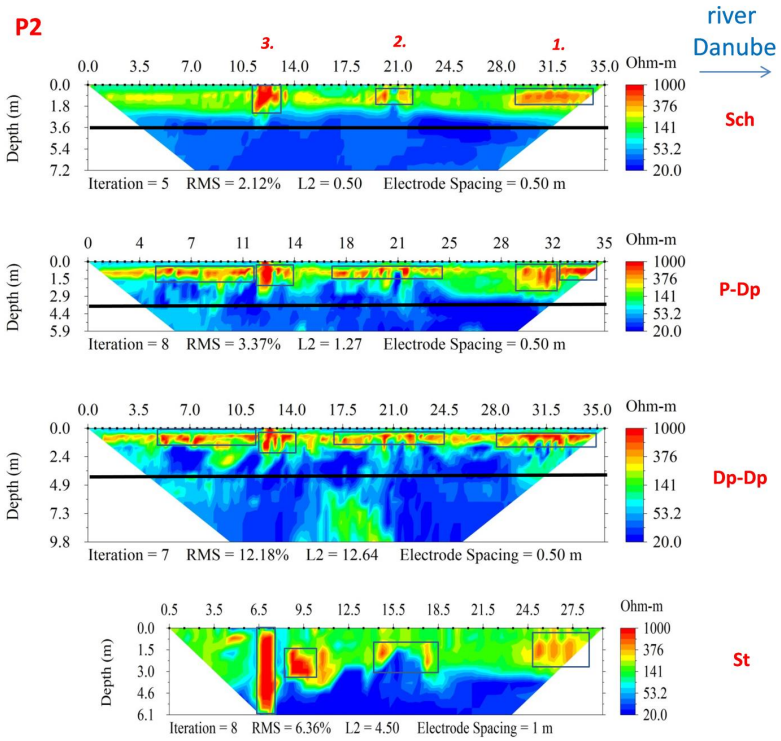

Figure 8. Deep section of the Schlumberger (Sch), Pole-Dipole (P-DP), Dipole-Dipole (Dp-Dp) and Stummer (St) arrays on P2. Rectangles delineate fractured zones. Red numbers are the zone numbers.

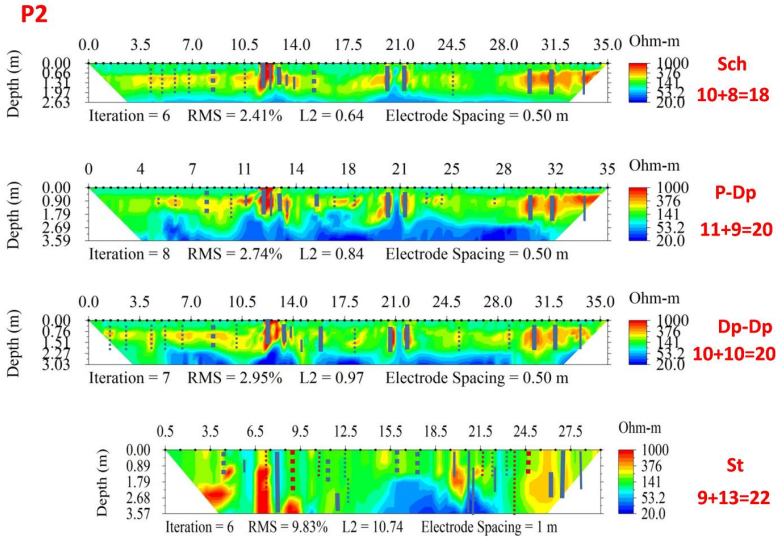

Figure 9. Shallow section of the Schlumberger (Sch), Pole-Dipole (P-DP), Dipole-Dipole (Dp-Dp) and Stummer (St) arrays on P2. Continues lines refer to fractures with high, dotted lines to fractures with small certainity. The numbers in the right side are their numbers for the section in the same row, accordingly.

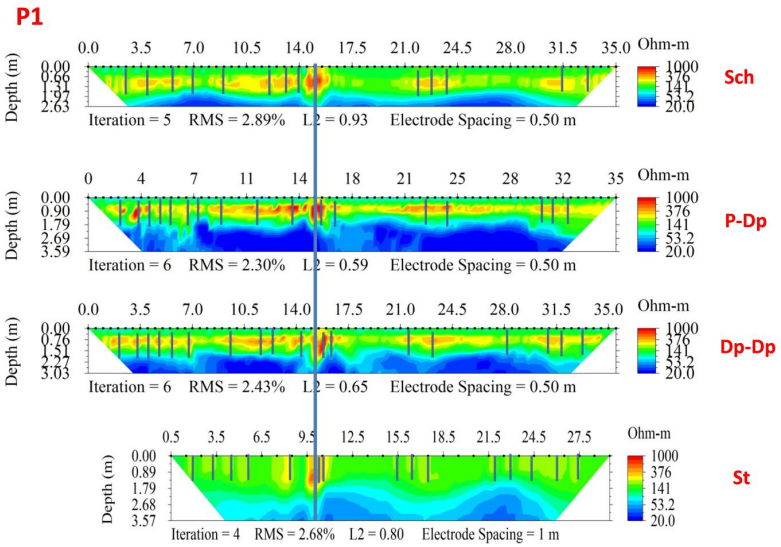

Figure 10. Schlumberger (Sch), Pole-Dipole (P-DP), Dipole-Dipole (Dp-Dp) and Stummer (St) array results on P1. Continues lines refer to fractures with high, dotted lines to fractures with small certainity. The long continues line presents the main fracture (MF).

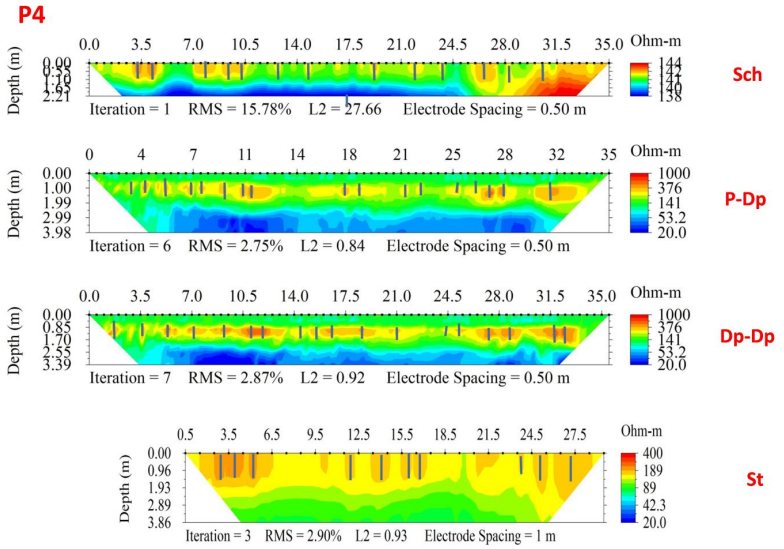

Figure 11. Schlumberger (Sch), Pole-Dipole (P-DP), Dipole-Dipole (Dp-Dp) and Stummer (St) array results on P4. Continues lines refer to fractures with high, dotted lines to fractures with small certainity.

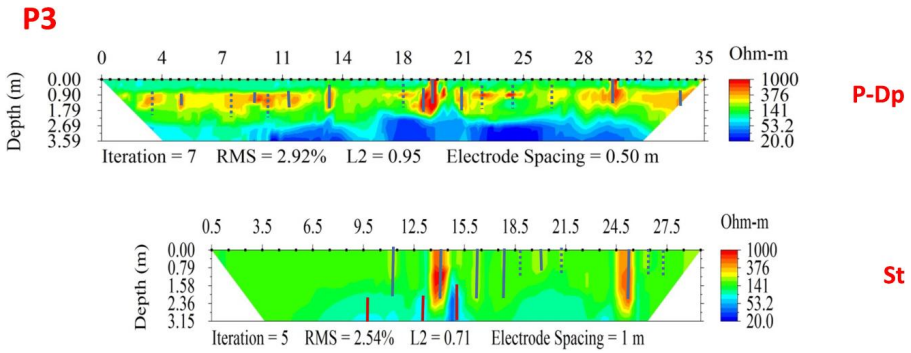

Figure 12. Schlumberger (Sch) and Pole-Dipole (P-DP) array results on P3. Continues lines refer to fractures with high, dotted lines to fractures with small certainity.

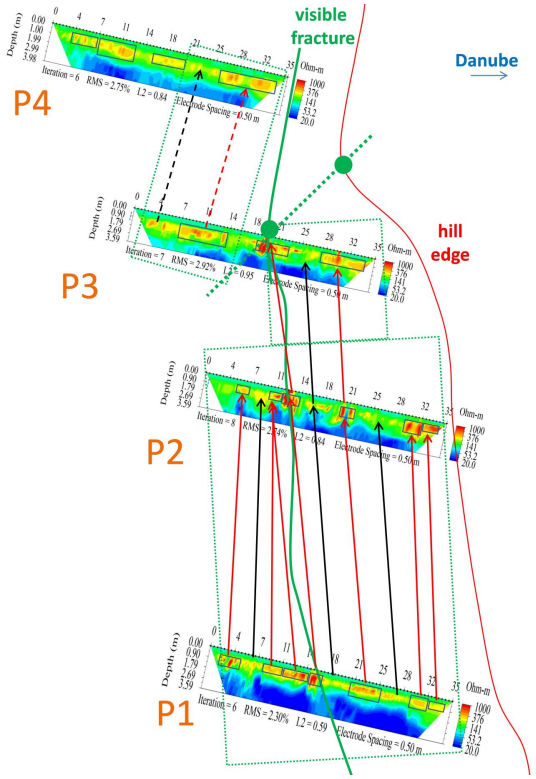

Figure 13. All Pole-Dipole (P-DP) profiles on the map of the study area. Continuous line rectangles delineate fractured zones. Dotted line rectangles delineate zones with the same fracture direction. Red arrows connect the coherent fracture zones, black arrays the stabile zones.

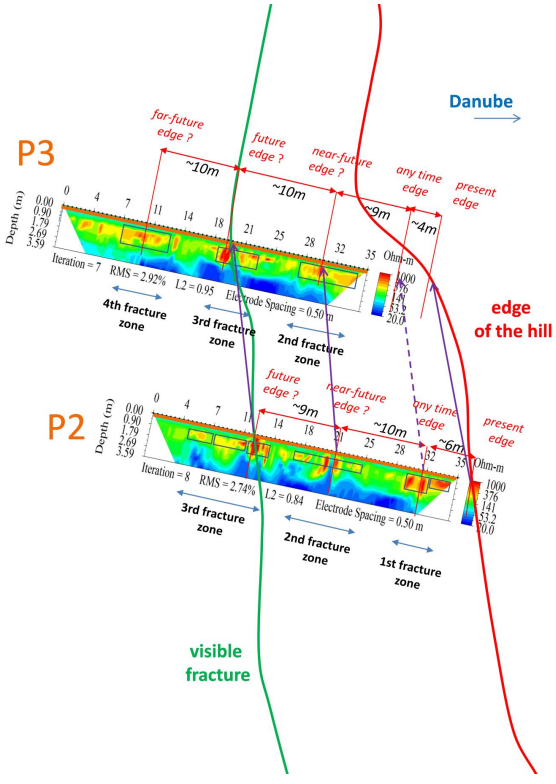

Figure 14. Central part of the study area with structural explanation. Continuous line rectangles delineate fractured zones. Purple arrows connect supposed coherent edges. The one is dotted because it is not on one of the sections.